Increase of Tumor Infiltrating γδ T-cells in Pancreatic Ductal Adenocarcinoma Through Remodeling of the Extracellular Matrix by a Hyaluronan Synthesis Suppressor, 4-Methylumbelliferone

(4–メチルウンベリフェロンによる膵癌間質抑制は腫瘍浸潤γδT細胞を増加させる)

申　請　者　　弘前大学大学院医学研究科

腫瘍制御科学領域消化器外科学教育研究分野

氏　　名　　須藤　亜希子

指導教授　　袴田　健一

Abstract

Objectives: Desmoplastic changes of extracellular matrix (ECM) containing large amounts of hyaluronan (HA) are of interest in chemo- and immunoresistance of pancreatic ductal adenocarcinoma (PDAC). The goal of this study was to evaluate the effects of 4-methylumbelliferone (MU), a selective inhibitor of HA, on ECM and to examine how MU affects adoptive immunotherapy.

Methods: The effect of MU on cell proliferation, HA synthesis and formation of ECM were investigated in four PDAC cell lines. In addition, the cytotoxicity of γδ T-cell-rich peripheral blood mononuclear cells (PBMCs) collected from healthy donors and stimulated with zoledronate and interleukin-2 was examined in the presence of MU. The amount of HA and tumor-infiltrating lymphocytes were also investigated in mice xenograft models.

Results: *In vitro*, 1.0 mM MU inhibited cell proliferation by 45-70% and HA synthesis by 55-80% in all four PDAC cell lines, and enhanced γδ T-cell-rich PBMC-mediated cytotoxicity against PDAC cells. *In vivo*, MU reduced intratumoral HA and promoted infiltration of inoculated γδ T-cells into tumor tissue, and consequently suppressed tumor growth.

Conclusions: MU may be an effective immunosensitizer against PDAC through induction of structural changes in the ECM.

Key Words: pancreatic cancer, 4-methylumbelliferone, extracellular matrix, hyaluronan, γδ T-cell

Introduction

Pancreatic ductal adenocarcinoma (PDAC) is a malignant neoplasm with a 5-year survival rate of less than 10% [1]. Several factors contribute to this poor prognosis, including late diagnosis due to PDAC patients having no specific symptoms, the high malignant potential of PDAC cells, and chemo- and immunoresistance due to desmoplastic change of the extracellular matrix (ECM), which contains a large amount of hyaluronan (HA) [2-7]. This HA-rich microenvironment is advantageous for cell proliferation and migration [8,9].

HA is a high molecular weight glycosaminoglycan that consists of repeated β-1,4-GlcUA-β-1,3-GlcNAc disaccharide units and is a ubiquitous macromolecule in the ECM [10]. HA biosynthesis universally occurs at HA synthases residing at the plasma membrane that catalyze transglycosylation from uridine diphosphate (UDP)-GlcUA and UDP- GlcNAc in eukaryotic cells [11,12]. HA synthesis in ECM formation in human skin fibroblasts is inhibited by 4-methylumbelliferone (MU) [13] as a result of depletion of UDP-GlcUA [14]. Thus, MU is of interest as an anticancer agent targeting HA in various cancers [15-20] and we have shown the anticancer activity of this compound in PDAC cells through inhibition of HA synthesis and ECM formation [21-25]. MU also enhances the anticancer activity of gemcitabine *in vivo* [21], and consequently MU is likely to promote the activity of immunocompetent cells.

Human γδ T-cells are an important reservoir in immunotherapy for cancer. Most human γδ peripheral blood lymphocytes express Vγ9Vδ2 T-cell receptor, which is specific for non-peptide phosphoantigens from tumor cells and microbes. The natural killer group 2D (NKG2D) receptor is even more important for tumor recognition. This receptor is expressed on all Vγ9Vδ2 T-cells and provides activation signals for cytolytic responses through expression of

cytotoxic molecules by binding to ligands such as non-classical major histocompatibility complex (MHC) proteins of the MHC class I chain-related molecules (MIC) MICA and MICB, and UL-16 binding proteins expressed on the surface of infected or tumor cells [26-30]; for instance, pancreatic cancer tissues express more MICA compared to inflammatory and normal pancreatic tissues [31].

Several clinical trials have investigated the safety and efficacy of γδ T-cell-based immunotherapy [32,33] and combination therapy with gemcitabine in patients with curatively resected PDAC [34]. However, the interaction between MU and γδ T-cell-based immunotherapy in PDAC remains unclear. Therefore, the objective of this study is to evaluate the effects of MU on immunotherapy using γδ T-cells against PDAC.

Materials and Methods

Materials

4-Methylumbelliferone and *Streptomyces* hyaluronidase were purchased from Wako Pure Chemicals (Osaka, Japan). Actinase E was purchased from Kaken Pharmaceutical Co. (Tokyo, Japan). All other reagents were of analytical grade and were obtained from commercial sources.

Cell Lines and Reagents

Four PDAC cell lines, AsPC-1, BxPC-3 (DS Pharma Biomedical Co., Osaka, Japan), PANC-1 (RIKEN BRC Cell Bank, Tsukuba, Japan), and MIA PaCa-2 (a kind gift from the Department of Pharmacy, Hirosaki University Hospital, Hirosaki, Japan), were used in the study.

Cells were grown as monolayers at 37°C in a 5% CO_2 atmosphere in Dulbecco's modified Eagle's medium (DMEM) (MIA PaCa-2) (Nacalai Tesque Inc., Kyoto, Japan) or RPMI-1640 (AsPC-1, BxPC-3 and PANC-1) (Thermo Fisher Scientific, Kanagawa, Japan) supplemented with 10% heat-inactivated fetal bovine serum, L-glutamine, sodium pyruvate, 100 μg/mL streptomycin, 100 IU/mL penicillin, and 0.25 μg/mL amphotericin B.

Mice

NOD/ShiJic-scid jcl mice were purchased from Japan Clea (Tokyo, Japan). The mice were housed under specific pathogen-free conditions with controlled light-dark cycles, temperature and humidity, and water and food *ad libitum* to reduce stress on the animals. The mice were used in the study at 7 weeks of age and at a weight of approximately 25 g. All animal experiments were performed according to the Guidelines for Animal Experimentation of Hirosaki University.

Expansion of human peripheral blood γδ T-cells

Preparation of γδ T-cell-rich peripheral blood mononuclear cells (PBMCs) was performed with reference to a previous article [35]. Up to 50 mL of peripheral blood was obtained from healthy volunteers following written informed consent and approval by the institutional research ethics committee. PBMCs were isolated using a Leucosep (Greiner Bio-One International GmbH, Kremsmunster, Austria) and resuspended at $1x10^6$ cells/mL in RPMI-1640 supplemented with 10% heat-inactivated fetal bovine serum, L-glutamine, sodium pyruvate, 25 mM HEPES, 100 μg/mL streptomycin, 100 IU/mL penicillin, and 0.25 μg/mL amphotericin B.

Human interleukin-2 (IL-2; Sigma-Aldrich, Darmstadt, Germany) and zoledronate (Zometa; AdooQ BioScience, Irvine, Calif, USA) were added to final concentrations of 1000 IU/mL and 5 μM, respectively. IL-2 (100 IU/mL) was added every 2 days over the culture period. After 14 days, samples were analyzed on a flow cytometer (FACSAria II; BD Biosciences, San Jose, Calif, USA) to evaluate expansion of the γδ T-cells. PE-conjugated antibody to TCRVγ9 and APC-conjugated antibody to CD3 were purchased from BD Biosciences.

Proliferation assay

Cells ($1x10^5$ cells/well) were seeded on 6-well plates (Iwaki; Analytical Technologies Group, LLC, Groton, Conn, USA). After incubation for 24 h, serial concentrations of MU dissolved in dimethyl sulfoxide (DMSO; Wako Pure Chemicals, Osaka, Japan) were added. After incubation for 48 h, adhesive cells were removed using trypsin, resuspended in phosphate-buffered saline (PBS), and counted using an automated cell counter (TC20; Bio-Rad, Tokyo, Japan).

Particle exclusion assay

Pericellular matrices were visualized using a particle exclusion assay [36]. Fixed horse erythrocytes (Nippon Biotest Laboratories Inc., Tokyo, Japan) were reconstituted in PBS at $5x10^8$ cells/mL. Cells were cultured in 100-mm dishes. After incubation for 24 h, serial dilutions of MU were added. Following incubation for 48 h, the pericellular matrix was visualized by adding the horse erythrocyte suspension to the dishes and viewing under a light microscope. To show that the pericellular matrix was composed of HA, MU-free dishes were

preincubated for 2 h with 1.0 U/mL *Streptomyces* hyaluronidase (HYAL) prior to the assay. Quantification of the halo area was carried out using Image J software (US National Institutes of Health, Bethesda, Md, USA).

HA staining of PDAC cells

Slide glasses (Matsunami Glass IND., Osaka, Japan) were sterilized by overnight exposure to UV light in 100-mm dishes. Cells ($1x10^5$ cells/dish) were cultured in the dish and incubated. After incubation for 24 h, serial dilutions of MU were added. Following incubation for 48 h, cells were washed twice with PBS, fixed with 4% paraformaldehyde buffered with PBS at room temperature for 2 h, and rinsed twice with PBS. Following antigen retrieval, tissue samples were incubated for 32 min at 37°C with 25 μg/mL biotinylated HA binding protein (HABP; catalog no., BC41; Hokudo Co., Osaka, Japan). Streptavidin horseradish peroxidase conjugate and 3,3′-diaminobenzidine (DAB) from the iVIEW DAB universal kit (Ventana Medical Systems, Tucson, Ariz, USA) were used to visualize the results. Negative controls were stained with HABP following digestion of the tissue sections with 1.0 U/mL *Streptomyces* HYAL.

Analysis of HA synthesis in PDAC cells

Cells ($1x10^5$ cells/well) were seeded on 6-well plates. After incubation for 24 h, serial concentrations of MU were added. After incubation for 48 h, the medium was withdrawn and centrifuged to remove the cells. Supernatants were subjected to ethanol precipitation. HA in precipitates was dissolved in H_2O and quantified by an enzyme-linked binding protein assay kit

using a competition method (PG Research Co., Tokyo, Japan).

Cytotoxicity assay

Cells ($5x10^4$ cells/well) were seeded on 6-well plates. After incubation for 24 h, 1.0 mM MU was added. After incubation for 48 h, adhesive cells were counted and then an appropriate number of γδ T-cell-rich PBMCs adjusted to the desired effector/target (E/T) ratio were added to each well supplemented with 100 U/mL IL-2. After incubation for a further 24 h, the medium containing floating cells was removed, and adhesive cells were washed twice with PBS, removed using trypsin, and resuspended in PBS. Viable cells were then counted using trypan blue solution. The cytotoxicity of γδ T-cells against PDAC cells was defined using the percentage viability for each group, which was calculated with the following formula: survival rate (%) = $N_{sample}/N_{control}$ x 100, where N_{sample} and $N_{control}$ are the number of viable cells in the control and sample groups, respectively.

Perforin ELISA

PDAC cells ($5x10^4$ cells/well) were seeded on 6-well plates. After incubation for 72 h, the cells were counted and then an appropriate number of γδ T-cell-rich PBMCs adjusted to the desired E/T ratio were added to each well supplemented with 100 U/mL IL-2. After incubation for a further 24 h, the medium was withdrawn and centrifuged to remove the cells, and perforin was quantified using a sandwich enzyme-linked protein assay kit (Arigo Biolaboratories Corp., Hsinchu, Taiwan).

Western blotting

Cells ($1x10^5$ cells/well) were seeded on 6-well plates. After incubation for 24 h, 1.0 mM MU was added. After incubation for 48 h, cells were prepared by dissolving cell pellets directly in sample buffer (62.5 mM Tris-HCl; pH 6.8, 2% SDS, and 10% glycerol). Protein concentrations were quantified using a bicinchoninic acid protein assay kit (Thermo Fisher Scientific, Waltham, Mass, USA). After protein quantification, 5 μg of protein per lane was separated by 8% SDS-PAGE and transferred onto a polyvinylidene difluoride (PVDF) membrane (Millipore, Billerica, Mass, USA). The membrane was blocked with 1% skim milk-PBS with 0.1% Tween 20 (PBST) and blotted with anti-MICA antibody (Abcam, Cambridge, England). After washing with PBST, the membrane was incubated with horseradish peroxidase-conjugated secondary antibody and visualized using ImmunoStar chemiluminescent reagent (Wako Pure Chemicals, Osaka, Japan).

Tumor inoculation

A suspension of $5x10^5$ BxPC-3 cells was subcutaneously injected into the dorsal region of mice. Two weeks later, mice were randomized into groups treated without MU (controls) or with MU orally administered at a dose of 2 mg/g body weight every day, mixed with bait to reduce stress on the animals. After a further two weeks, mice received intraperitoneal injection of previously expanded γδ T-cell-rich PBMCs ($1x10^7$ cells/body) from one donor. Treatments were repeated weekly for a total of 4 weeks. Once a week, tumor size was compared between the MU-treated and control groups using a caliper. The tumor volume was calculated as length x width^2 x 0.52 [37].

Analysis of HA synthesis in pancreatic cancer tissue

Mice were euthanized at a humane endpoint and tumors were removed. The dry weight of each tumor was measured after desiccation at 60°C for 4 h. Each sample was minced and digested overnight at 55°C with 0.25% actinase E/10 mM Tris-HCl (1ml; pH 8.0), followed by incubation at 100°C for 10 min to terminate the reaction. Upon centrifugation, supernatant containing HA was collected and subjected to ethanol precipitation. HA in precipitates was dissolved in H_2O and quantified using a hyaluronan quantification kit, as described above.

HA staining of tumor tissues

Removed tumors were fixed in 10% formalin (Wako Pure Chemicals, Osaka, Japan) and placed in 70% ethanol and 5% glacial acetic acid. Samples were embedded in paraffin using routine procedures, sliced at a thickness of 4 μm, and analyzed using an iVIEW DAB universal kit. Antigen retrieval was conducted using cell conditioning solution (CC1-Tris based EDTA buffer; pH 8.0; Ventana Medical Systems) and tissue samples were incubated for 32 min at 37°C with 25 μg/mL biotinylated HABP.

Analysis of tumor-infiltrating lymphocytes

Removed tumors were fixed and embedded in paraffin using routine procedures, sliced at a thickness of 4 μm, and analyzed using an iVIEW DAB universal kit. Antigen retrieval was conducted using cell conditioning solution and tissue samples were incubated for 32 min at 37°C with Monoclonal Mouse Anti-Human CD3 (Dako A/S, Glostrup, Denmark). The iVIEW

DAB Universal kit was used to visualize the results. To evaluate tumor-infiltrating lymphocytes, the mean number of CD3-positive cells per high-power field (HPF) was counted after random sampling of 10 areas within 1000 μm from the invasive front of the tumor.

Statistical analysis

Statistical analysis was performed using a Steel test and Mann-Whitney U test. Differences with $P < 0.05$ were considered to be significant.

Results

MU inhibits proliferation of PDAC cells

MU inhibited cell proliferation of all 4 PDAC cell lines in a dose-dependent manner (Fig. 1). After incubation with 1.0 mM MU for 48 h, proliferation of BxPC-3, PANC-1, AsPC-1 and MIA PaCa-2 cells was significantly inhibited by 65%, 70%, 69% and 45%, respectively (all $P < 0.05$).

MU reduces HA synthesis and pericellular HA matrices in PDAC cells

Treatment with MU resulted in a significant decrease in HA synthesis in PDAC cells, as previously reported [21,22,24,25,38]. Immunohistochemical staining for HA indicated that all four PDAC cell lines retained HA on their cell surface, but cells incubated with MU showed weak HA expression (Fig. 2A). HA quantification showed that the MU-induced decline in HA retention was almost dose-dependent, and 1.0 mM MU caused 80% and 55% decreases of HA in BxPC-3 and PANC-1 cells, compared with controls ($P < 0.05$; Fig. 2C). The pericellular

matrix surrounding PDAC cells, which contains HA, was visualized using a particle exclusion assay. MU-treated PDAC cells had less pericellular matrix than non-treated cells (Fig. 2D). Evaluation of the ratio of the pericellular matrix area to the nuclear area showed that MU and HYAL significantly decreased the area of HA-containing pericellular matrix ($P < 0.05$; Fig. 2B).

MU enhances γδ T-cell-rich PBMC-mediated cytotoxicity against PDAC cells

The cytotoxicity of γδ T-cell-rich PBMCs expanded before examination was positively correlated with the increase in the E/T ratio (Fig. 3A). The % survival of PDAC cells preincubated with MU was 30%, 14%, 32% and 25% for BxPC-3, PANC-1, AsPC-1 and MIA PaCa-2 cells, respectively, at an E/T ratio of 20, and was significantly lower compared with controls (all $P < 0.05$). To study the mechanism of MU-induced enhancement of cytotoxic activity of γδ T-cells, release of perforin in cytolytic granules from expanded γδ T-cells and expression of MICA in PDAC cells were examined. Release of perforin was measured by ELISA, and expression of MICA was detected by Western blotting in all four cell lines (data not shown).

MU suppresses tumor growth and HA, and increases infiltrating lymphocytes

Based on *in vitro* experiments showing that BxPC-3 cells contain a large amount of HA that is strongly suppressed by MU, these cells were selected to investigate the efficacy of MU on treatment of PDAC with γδ T-cell-rich PBMCs *in vivo*. The tumor volume in γδ T-cell-rich PBMC-injected mice was 1.18 cm^3 in the MU-treated group compared to 1.59 cm^3 in the untreated group (Fig. 4A), showing significant suppression of tumor growth by treatment with a

combination of MU and γδ T-cell-rich PBMCs ($P < 0.05$). There was no significant difference in tumor growth between untreated and MU-treated mice without injection of γδ T-cell-rich PBMCs (data not shown). In addition, tumor staining showed that HA retention in the MU-treated group was lower than that in the untreated group, and the amount of HA in tumors was significantly reduced in the MU-treated group (Fig. 4B, C). MU also significantly increased the number of CD3-positive cells infiltrated into tumors ($P < 0.05$; Fig. 4D, E).

Discussion

In this study, growth of xenograft tumors was significantly suppressed by administration of a combination of MU and γδ T-cell-rich PBMCs *in vivo*. The amount of HA in tumors was decreased, while infiltration of CD3-positive cells into tumor tissues was significantly increased. These results show that orally administered MU can reach tumors, and moreover, that intra-abdominally injected γδ T-cell-rich PBMCs can also distribute to the tumors, resulting in inhibition of tumor growth. This conclusion is reached because NOD/ShiJic-scid jcl mice have loss of endogenous functional T- and B-cells.

A structural weakness of gaps between pancreatic tumor cells induced by MU may cause a synergistic effect of anticancer agents or immunocompetent lymphocytes [24]. MU enhances the anticancer activity of gemcitabine against PDAC *in vivo* [21] and other treatment targeting HA can also sensitize the effects of chemotherapeutic agents owing to normalization of the elevated interstitial pressure in PDAC tissues [39,40]. Additionally, MU reduces the amount of tumoral HA, leading to a decrease in tumor interstitial pressure, and boosts the number of cytotoxic T lymphocytes in murine colorectal carcinoma [41]. This remodeling of the tumor

microenvironment through a decrease in HA seems to be advantageous for the effects of immunocompetent cells against PDAC.

PDAC cells treated with MU had poorer survival compared to non-treated cells when incubated with γδ T-cell-rich PBMCs *in vitro.* Perforin from the cytotoxic cells was detected in the culture medium by ELISA, and expression of MICA was detected by Western blot analysis. These results suggest that expanded γδ T-cells have cytolytic activity against PDAC cells. Some drugs increase expression of NKG2D ligands to enhance immunocompetence against a tumor [42,43], but cells treated with MU showed variable (higher or lower) expression of MICA compared with non-treated cells, with no particular trend in the four PDAC cell lines treated with MU. Subsequent analysis of HA synthesis showed that MU decreased the amount of HA and suppressed the visualized pericellular matrices in PDAC cells, consistent with previous reports [21-25]. Since there is no correlation between MU treatment and MICA expression, these results suggest that γδ T-cell-mediated cytotoxicity against PDAC cells is enhanced through a decrease in the HA coating on the cell surface, rather than an increase in MICA expression.

Targeting of HA appears to be a viable therapeutic strategy in PDAC, but there are several limitations in use of a combination of MU and γδ T-cell immunotherapy. First, MU has been used clinically as a choleretic agent with demonstrated safety [44], but has not been used as an anticancer agent in clinical settings. Therefore, further studies will be necessary to determine the dosing regimen and side effects of MU. Second, HA synthesized by T-cells themselves is critical for their IL-2-mediated proliferation, and MU inhibited mitogen-induced T-cell proliferation, although did not impair T cell activation [45]. While γδ T-cells from PBMCs can be expanded in *ex vivo*, it is unclear if PBMCs obtained from patients could be cultured without an

effect of MU. For example, PBMCs from some donors fail to respond to zoledronate stimulation [35], and new methods are needed to expand γδ T-cells, including expansion from induced pluripotent stem cells.

In conclusion, MU has anticancer properties in PDAC cell lines and enhances anticancer activity of γδ T-cell immunotherapy in xenograft models of PDAC. These results suggest that MU may be a candidate as a novel therapeutic agent for treatment of pancreatic cancer owing to its immunosensitizer properties.

Acknowledgements

The Authors would like to thank Professor Hiroshi Kijima and Dr. Satoko Morohashi (Department of Pathology and Bioscience, Hirosaki University, Graduate School of Medicine) for their excellent technical help, and Professor Akio Nakane (Department of Microbiology and Immunology, Hirosaki University, Graduate School of Medicine) for technical advice on experiments.

References

1. Siegel RL, Miller KD, Jemal A. Cancer statistics, 2016. *CA Cancer J Clin.* 2016;66:7-30.
2. Cheng XB, Sato N, Kohi S, et al. Prognostic impact of hyaluronan and its regulators in pancreatic ductal adenocarcinoma. *PloS one.* 2013;8:e80765.
3. Heldin CH, Rubin K, Pietras K, et al. High interstitial fluid pressure - an obstacle in cancer therapy. *Nat Rev Cancer.* 2004;4:806-813.
4. McBride WH, Bard JB. Hyaluronidase-sensitive halos around adherent cells. Their role in blocking lymphocyte-mediated cytolysis. *J Exp Med*. 1979;149:507-515.
5. Liu H, Ma Q, Xu Q, et al. Therapeutic potential of perineural invasion, hypoxia and desmoplasia in pancreatic cancer. *Curr Pharm Des.* 2012;18:2395-2403.
6. Theocharis AD, Tsara ME, Papageorgacopoulou N, et al. Pancreatic carcinoma is characterized by elevated content of hyaluronan and chondroitin sulfate with altered disaccharide composition. *Biochim Biophys Acta.* 2000;1502:201-206.
7. Kudo D, Suto A, Hakamada K. The Development of a Novel Therapeutic Strategy to Target Hyaluronan in the Extracellular Matrix of Pancreatic Ductal Adenocarcinoma. *Int J Mol Sci.* 2017;18.
8. Laurent TC, Fraser JR. Hyaluronan. *FASEB j.* 1992;6:2397-2404.
9. McDonald JA, Camenisch TD. Hyaluronan: genetic insights into the complex biology of a simple polysaccharide. *Glycoconj J.* 2002;19:331-339.
10. Weissmann B, Meyer K. The Structure of Hyalobiuronic Acid and of Hyaluronic Acid from Umbilical Cord1,2. *J Am Chem Soc.* 1954;76:1753-1757.
11. Weigel PH, Hascall VC, Tammi M. Hyaluronan synthases. *J Biol Chem.*

1997;272:13997-14000.

12. Tammi MI, Day AJ, Turley EA. Hyaluronan and homeostasis: a balancing act. *J Biol Chem.* 2002;277:4581-4584.
13. Nakamura T, Takagaki K, Shibata S, et al. Hyaluronic-acid-deficient extracellular matrix induced by addition of 4-methylumbelliferone to the medium of cultured human skin fibroblasts. *Biochem Biophys Res Commun.* 1995;208:470-475.
14. Kakizaki I, Kojima K, Takagaki K, et al. A novel mechanism for the inhibition of hyaluronan biosynthesis by 4-methylumbelliferone. *J Biol Chem.* 2004;279:33281-33289.
15. Yoshihara S, Kon A, Kudo D, et al. A hyaluronan synthase suppressor, 4-methylumbelliferone, inhibits liver metastasis of melanoma cells. *FEBS Lett.* 2005;579:2722-2726.
16. Kudo D, Kon A, Yoshihara S, et al. Effect of a hyaluronan synthase suppressor, 4-methylumbelliferone, on B16F-10 melanoma cell adhesion and locomotion. *Biochem Biophys Res Commun.* 2004;321:783-787.
17. Briggs A, Rosenberg L, Buie JD, et al. Antitumor effects of hyaluronan inhibition in desmoid tumors. *Carcinogenesis.* 2015;36:272-279.
18. Yates TJ, Lopez LE, Lokeshwar SD, et al. Dietary supplement 4-methylumbelliferone: an effective chemopreventive and therapeutic agent for prostate cancer. *J Natl Cancer Inst.* 2015;107.
19. Piccioni F, Fiore E, Bayo J, et al. 4-Methylumbelliferone inhibits hepatocellular carcinoma growth by decreasing IL-6 production and angiogenesis. *Glycobiology.* 2015;25:825-835.
20. Ikuta K, Ota T, Zhuo L, et al. Antitumor effects of 4-methylumbelliferone, a hyaluronan

synthesis inhibitor, on malignant peripheral nerve sheath tumor. *Int J Cancer.* 2017;140:469-479.

21. Nakazawa H, Yoshihara S, Kudo D, et al. 4-methylumbelliferone, a hyaluronan synthase suppressor, enhances the anticancer activity of gemcitabine in human pancreatic cancer cells. *Cancer Chemother Pharmacol.* 2006;57:165-170.
22. Morohashi H, Kon A, Nakai M, et al. Study of hyaluronan synthase inhibitor, 4-methylumbelliferone derivatives on human pancreatic cancer cell (KP1-NL). *Biochem Biophys Res Commun.* 2006;345:1454-1459.
23. Hajime M, Shuichi Y, Makoto N, et al. Inhibitory effect of 4-methylesculetin on hyaluronan synthesis slows the development of human pancreatic cancer in vitro and in nude mice. *Int J Cancer.* 2007;120:2704-2709.
24. Yoshida E, Kudo D, Nagase H, et al. Antitumor effects of the hyaluronan inhibitor 4-methylumbelliferone on pancreatic cancer. *Oncol Lett.* 2016;12:2337-2344.
25. Nagase H, Kudo D, Suto A, et al. 4-Methylumbelliferone Suppresses Hyaluronan Synthesis and Tumor Progression in SCID Mice Intra-abdominally Inoculated With Pancreatic Cancer Cells. *Pancreas.* 2017;46:190-197.
26. Nedellec S, Bonneville M, Scotet E. Human Vgamma9Vdelta2 T cells: from signals to functions. *Semin Immunol.* 2010;22:199-206.
27. Gomes AQ, Martins DS, Silva-Santos B. Targeting gammadelta T lymphocytes for cancer immunotherapy: from novel mechanistic insight to clinical application. *Cancer Res.* 2010;70:10024-10027.
28. Bauer S, Groh V, Wu J, et al. Activation of NK cells and T cells by NKG2D, a receptor for

stress-inducible MICA. *Science.* 1999;285:727-729.

29. Wu J, Song Y, Bakker AB, et al. An activating immunoreceptor complex formed by NKG2D and DAP10. *Science.* 1999;285:730-732.
30. Deng X, Terunuma H, Terunuma A, et al. Ex vivo-expanded natural killer cells kill cancer cells more effectively than ex vivo-expanded gammadelta T cells or alphabeta T cells. *Int immunopharmacol.* 2014;22:486-491.
31. Duan X, Deng L, Chen X, et al. Clinical significance of the immunostimulatory MHC class I chain-related molecule A and NKG2D receptor on NK cells in pancreatic cancer. *Med Oncol.* 2011;28:466-474.
32. Sakamoto M, Nakajima J, Murakawa T, et al. Adoptive immunotherapy for advanced non-small cell lung cancer using zoledronate-expanded gammadeltaTcells: a phase I clinical study. *J Immunother.* 2011;34:202-211.
33. Abe Y, Muto M, Nieda M, et al. Clinical and immunological evaluation of zoledronate-activated Vgamma9gammadelta T-cell-based immunotherapy for patients with multiple myeloma. *Exp Hematol.* 2009;37:956-968.
34. Aoki T, Matsushita H, Hoshikawa M, et al. Adjuvant combination therapy with gemcitabine and autologous gammadelta T-cell transfer in patients with curatively resected pancreatic cancer. *Cytotherapy.* 2017;19:473-485.
35. Kondo M, Izumi T, Fujieda N, et al. Expansion of human peripheral blood gammadelta T cells using zoledronate. *J Vis Exp.* 2011.
36. Evanko SP, Angello JC, Wight TN. Formation of hyaluronan- and versican-rich pericellular matrix is required for proliferation and migration of vascular smooth muscle cells.

Arterioscler, thromb Vasc Biol. 1999;19:1004-1013.

37. Andarini S, Kikuchi T, Nukiwa M, et al. Adenovirus vector-mediated in vivo gene transfer of OX40 ligand to tumor cells enhances antitumor immunity of tumor-bearing hosts. *Cancer Res.* 2004;64:3281-3287.
38. Cheng XB, Kohi S, Koga A, et al. Hyaluronan stimulates pancreatic cancer cell motility. *Oncotarget.* 2016;7:4829-4840.
39. Provenzano PP, Cuevas C, Chang AE, et al. Enzymatic targeting of the stroma ablates physical barriers to treatment of pancreatic ductal adenocarcinoma. *Cancer cell.* 2012;21:418-429.
40. Hingorani SR, Harris WP, Beck JT, et al. Phase Ib Study of PEGylated Recombinant Human Hyaluronidase and Gemcitabine in Patients with Advanced Pancreatic Cancer. *Clin Cancer Res.* 2016;22:2848-2854.
41. Malvicini M, Fiore E, Ghiaccio V, et al. Tumor Microenvironment Remodeling by 4-Methylumbelliferone Boosts the Antitumor Effect of Combined Immunotherapy in Murine Colorectal Carcinoma. *Mol Ther.* 2015;23:1444-1455.
42. Shi P, Yin T, Zhou F, et al. Valproic acid sensitizes pancreatic cancer cells to natural killer cell-mediated lysis by upregulating MICA and MICB via the PI3K/Akt signaling pathway. *BMC cancer.* 2014;14:370.
43. Wang WJ, Qin SH, Zhang JW, et al. Combination doxorubicin and interferon-alpha therapy stimulates immunogenicity of murine pancreatic cancer Panc02 cells via up-regulation of NKG2D ligands and MHC class I. *Asian Pac J Cancer Prev.* 2014;15:9667-9672.
44. Nagy N, Kuipers HF, Frymoyer AR, et al. 4-methylumbelliferone treatment and hyaluronan

inhibition as a therapeutic strategy in inflammation, autoimmunity, and cancer. *Front Immunol.* 2015;6:123.

45. Mahaffey CL, Mummert ME. Hyaluronan synthesis is required for IL-2-mediated T cell proliferation. *J Immunol.* 2007;179:8191-8199.

Figure Legends

Figure 1. Effects of MU on proliferation in PDAC cells. Each bar represents the mean ± of 5 replications. *$P < 0.05$.

Figure 2. Effects of MU on the HA synthesis and pericellular matrix in PDAC cells. A, Immunohistochemical staining of PDAC cells. The scale bar is 50 μm. B, The pericelluar matrix area/nuclear area was analyzed using Image J software. Each bar represents the mean ± SD of 3 experiments (30 cells analyzed per experiment). *$P < 0.05$. C, Effect of MU on the synthesis of HA. Each bar represents the mean ± SD of 5 replications. *$P < 0.05$. D, The pericellular matrix was visualized using a particle exclusion assay. The scale bar is 10 μm. (PANC-1)

Figure 3. The cytotoxic activities of γδ T-cell-rich PBMCs against PDAC cells. Data represent the mean of 5 independent assays. *$P < 0.05$.

Figure 4. Anticancer effects of MU and γδ T-cell-rich PBMCs *in vivo* using BxPC-3 cells. A, Size of the inoculated tumors. Data represent the mean of 3 mice. *$P < 0.05$. B, Immunohistochemical staining with HA-binding protein of tumors. The scale bar is 100 μm. C, Hyaluronan quantification of tumors. Each bar represents the mean ± SD. *$P < 0.05$. D, Anti-CD3 staining of tumors. The scale bar is 100 μm. E, The number of CD3-positive cells infiltrated into tumors. The bar represents the mean ± SD of 3 mice (10 HPF analyzed per tumor). *$P < 0.05$.

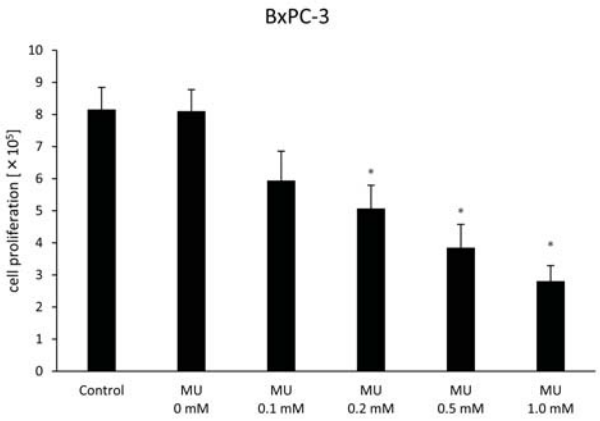
BxPC-3
cell proliferation [× 10⁵]
Control
MU 0 mM
MU 0.1 mM
MU 0.2 mM
MU 0.5 mM
MU 1.0 mM

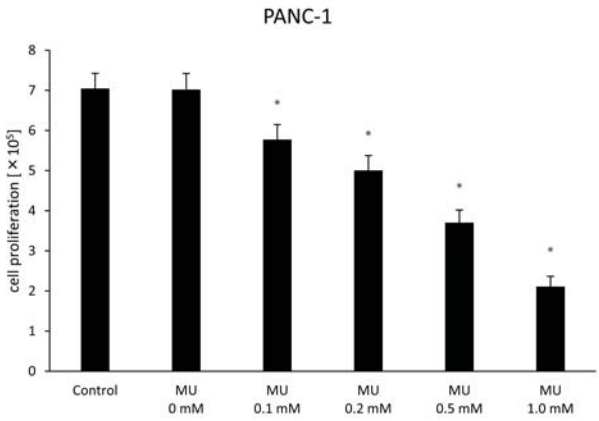
PANC-1
cell proliferation [× 10⁵]
Control
MU 0 mM
MU 0.1 mM
MU 0.2 mM
MU 0.5 mM
MU 1.0 mM

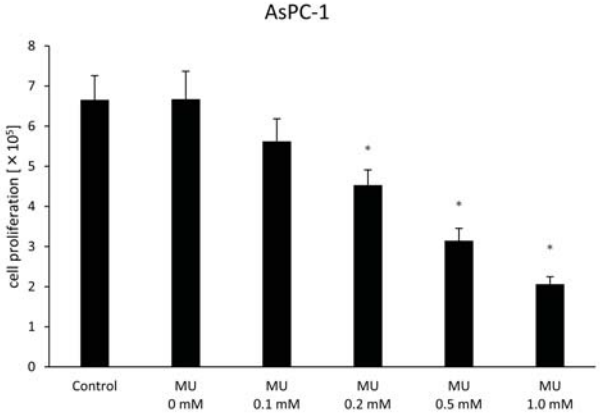
AsPC-1
cell proliferation [× 10⁵]
Control
MU 0 mM
MU 0.1 mM
MU 0.2 mM
MU 0.5 mM
MU 1.0 mM

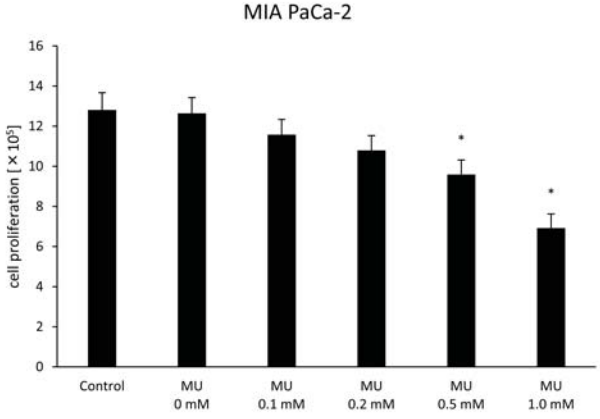
MIA PaCa-2
cell proliferation [× 10⁵]
Control
MU 0 mM
MU 0.1 mM
MU 0.2 mM
MU 0.5 mM
MU 1.0 mM

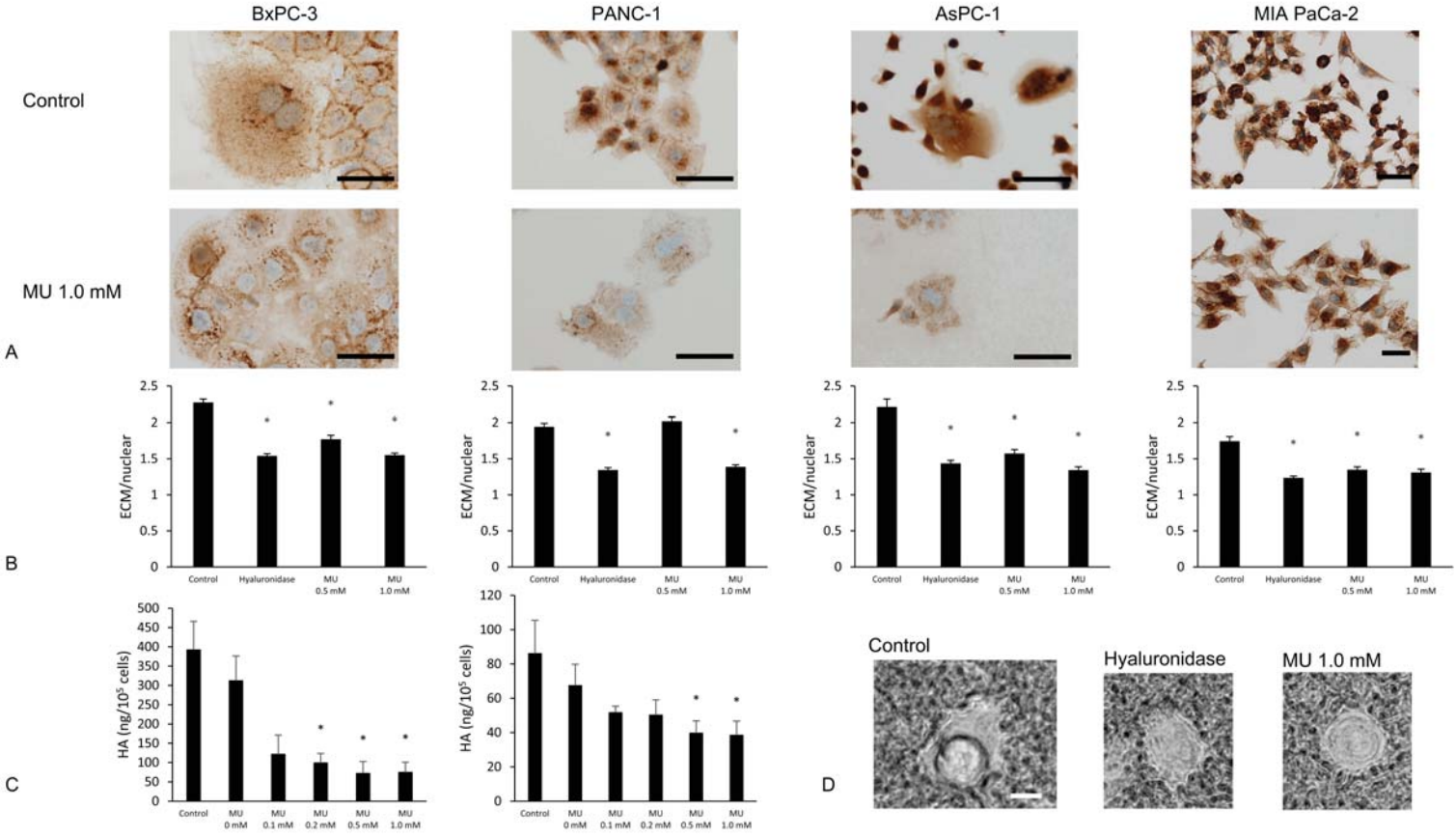
BxPC-3
PANC-1
AsPC-1
MIA PaCa-2
Control
MU 1.0 mM
A
B
C
D
ECM/nuclear
HA (ng/10^5 cells)
Control
Hyaluronidase
MU 0.5 mM
MU 1.0 mM
MU 0 mM
MU 0.1 mM
MU 0.2 mM

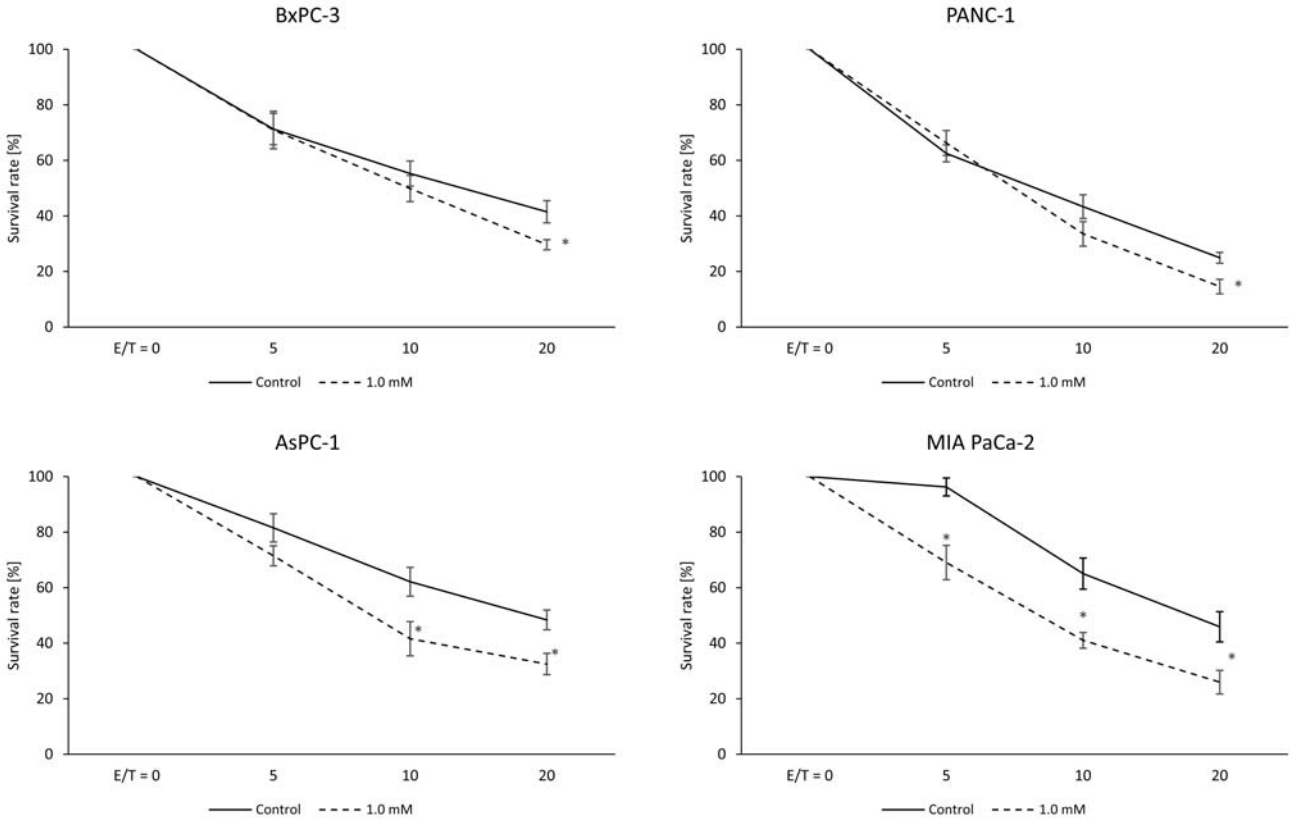
BxPC-3
PANC-1
AsPC-1
MIA PaCa-2
Survival rate [%]
100
80
60
40
20
0
E/T = 0
5
10
20
Control
1.0 mM
*

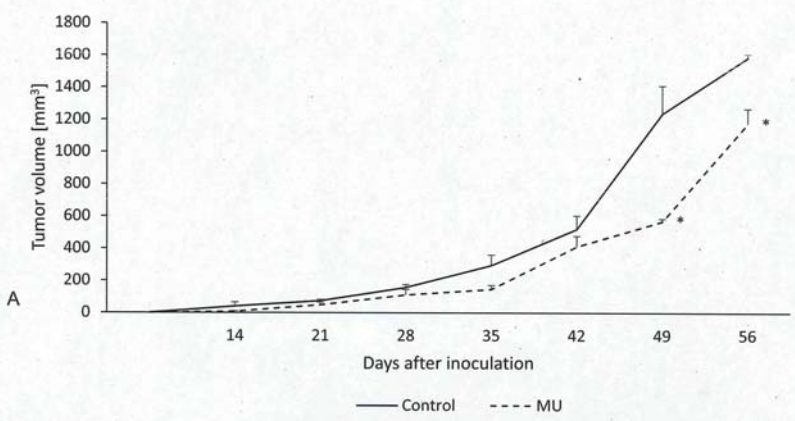
A
Tumor volume [mm³]
1800
1600
1400
1200
1000
800
600
400
200
0
14
21
28
35
42
49
56
Days after inoculation
Control
MU
*
*

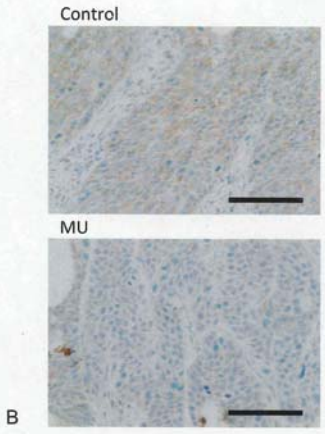
Control
MU
B

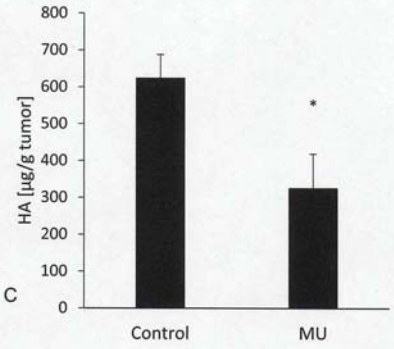
C
HA [µg/g tumor]
800
700
600
500
400
300
200
100
0
*
Control
MU

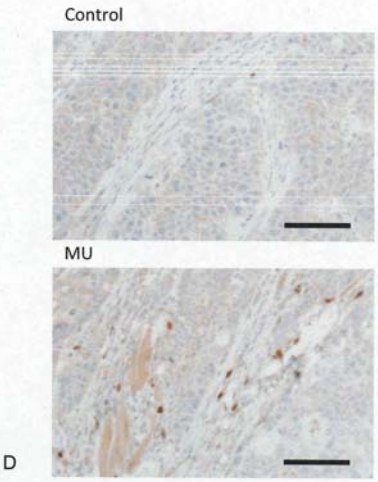
Control
MU
D

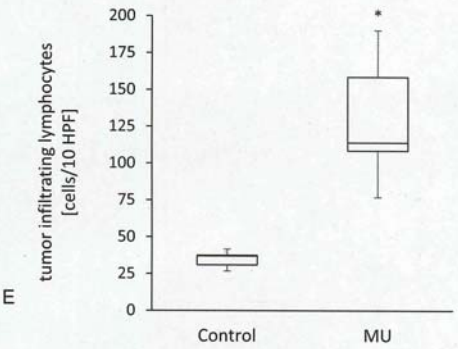
E
tumor infiltrating lymphocytes [cells/10 HPF]
200
175
150
125
100
75
50
25
0
*
Control
MU